Image-guided adaptive radiation therapy (IGART): Radiobiological and dose escalation considerations for localized carcinoma of the prostate

William Song[a)] and Bryan Schaly
Department of Medical Biophysics, University of Western Ontario, and Radiation Treatment Program, London Regional Cancer Program, London Health Sciences Centre, London, Ontario, Canada

Glenn Bauman
Department of Oncology, University of Western Ontario, and Radiation Treatment Program, London Regional Cancer Program, London Health Sciences Centre, London, Ontario, Canada

Jerry Battista and Jake Van Dyk
Departments of Medical Biophysics and Oncology, University of Western Ontario, and Radiation Treatment Program, London Regional Cancer Program, London Health Sciences Centre, London, Ontario, Canada

(Received 29 November 2004; revised 14 April 2005; accepted for publication 21 April 2005; published 15 June 2005)

The goal of this work was to evaluate the efficacy of various image-guided adaptive radiation therapy (IGART) techniques to deliver and escalate dose to the prostate in the presence of geometric uncertainties. Five prostate patients with 15–16 treatment CT studies each were retrospectively analyzed. All patients were planned with an 18 MV, six-field conformal technique with a 10 mm margin size and an initial prescription of 70 Gy in 35 fractions. The adaptive strategy employed in this work for patient-specific dose escalation was to increase the prescription dose in 2 Gy-per-fraction increments until the rectum normal tissue complication probability (NTCP) reached a level equal to that of the nominal plan NTCP (i.e., iso-NTCP dose escalation). The various target localization techniques simulated were: (1) daily laser-guided alignment to skin tattoo marks that represents treatment without image-guidance, (2) alignment to bony landmarks with daily portal images, and (3) alignment to the clinical target volume (CTV) with daily CT images. Techniques (1) and (3) were resimulated with a reduced margin size of 5 mm to investigate further dose escalation. When delivering the original clinical prescription dose of 70 Gy in 35 fractions, the "CTV registration" technique yielded the highest tumor control probability (TCP) most frequently, followed by the "bone registration" and "tattoo registration" techniques. However, the differences in TCP among the three techniques were minor when the margin size was 10 mm ($\leqslant$1.1%). Reducing the margin size to 5 mm significantly degraded the TCP values of the "tattoo registration" technique in two of the five patients, where a large difference was found compared to the other techniques ($\leqslant$11.8%). The "CTV registration" technique, however, did maintain similar TCP values compared to their 10 mm margin counterpart. In terms of normal tissue sparing, the technique producing the lowest NTCP varied from patient to patient. Reducing the margin size seemed the only sure way to reduce the NTCP significantly, irrespective of the IGART technique employed. In escalating the dose with the iso-NTCP constraint, the largest average gain in dose was observed with the "tattoo registration" technique, followed by the "CTV registration" and "bone registration" techniques. This is attributed to the fact that in three of the five patients, the "tattoo registration" technique yielded the lowest NTCP, hence a greater window of opportunity to escalate the dose was possible with this technique. However, the variation among the five patients was also largest with the "tattoo registration" technique where, in the case of one patient, the required dose actually needed to be below the original prescription dose of 70 Gy to satisfy the iso-NTCP constraint. This was not the case with the "CTV registration" technique where positive and similar dose escalation was allowed on all five patients. Based on these data, an attractive dose escalation strategy may be to implement the "CTV registration" technique (for consistent dosimetric coverage) for daily target localization in combination with a margin reduction (for increased normal tissue sparing). [DOI: 10.1118/1.1935775]

Key words: image-guided adaptive radiation therapy, iso-NTCP dose escalation, prostate cancer, tumor control probability, normal tissue complication probability

I. INTRODUCTION

The majority of new cases of prostate cancer are nonmetastatic and locally confined or regional.[1] Under these conditions dose escalation is an attractive strategy since well-contained tumors may allow more conformal dose distributions to be delivered, while avoiding critical struc-

tures. This feature, with the advent of three-dimensional conformal and intensity modulated radiation therapies (3DCRT and IMRT) and other imaging advances, has helped various institutions to increase the dose prescription beyond 70 Gy.[2–6] Thus far, with IMRT, it has been shown that a dose of up to 81 Gy can be administered safely with acceptable complication rates.[6]

Technically, a major limitation in our efforts to escalate dose further to the prostate is due to geometric uncertainties caused by organ motion/deformation of the target and critical structures and day-to-day set-up variations.[7–10] The deleterious effect of these uncertainties has been well documented and is considered a major impediment to further dose escalation.[11–17] As a result, the development of image-guided target localization[11,18–21] and patient-specific adaptation techniques,[12,14,22–27] collectively termed in this paper as image-guided adaptive radiation therapy (IGART), has become a major research focus in medical physics.[18]

Thus far, a variety of different IGART techniques have been proposed but since the concept is still in its infancy the reports on their efficacy in terms of dosimetric consequences and clinical outcomes are scarce. Happersett *et al.*[13] recently reviewed dose escalation in prostate treatments achieved with highly conformal IMRT and six-field techniques. They concluded that 81 Gy could be delivered while maintaining acceptable complication rates. However, they did not investigate how different image guidance technologies could affect their results. Martinez *et al.*[14] conducted a dose escalation study for prostate cancer by generating a confidence-limited PTV (introduced by Yan *et al.*[22]) using on-line portal and CT image data during the first week of treatment. An adaptive radiation therapy (ART) process devised in-house then determined the possible dose escalation. In this way, they showed that the average dose could be escalated by 5% (2.5%–10%) using four-field conformal radiation therapy (CRT) and 7.5% (2.5%–15%) using IMRT. These results showed that the achievable level of dose escalation using ART is highly patient dependent.

For the past several years, we have also been investigating and critically evaluating the effectiveness of new image guidance technologies through deformable model analysis in the prostate.[28–30] The main goal of the study was to quantify the dosimetric impact of localizing the target volume during a course of conformal radiotherapy, with the guidance of either laser-aligned skin tattoo marks, portal imaging of bones, and CT (or ultrasound) imaging of soft tissues.[30] Based on the results, we estimated the effects of these various modes of setup corrections on the treatment objectives.

In this work, we continue to evaluate the potential usefulness of image guidance technologies in terms of their ability to aid in the dose escalation to the prostate in combination with a patient-specific adaptive strategy of keeping late complications constant. Retrospective analysis of potential clinical benefits achieved, in terms of increased tumor control probability (TCP), is investigated when theoretical dose escalation is permitted while maintaining a constant normal tissue complication probability (i.e., iso-NTCP dose escalation), for treatment courses that are planned and delivered with the aid of various laser-guided and image-guided target localization techniques. The goal was to determine an optimum strategy for dose escalation in radiation therapy of the prostate cancer.

II. METHODS AND MATERIALS

A. Patient data and treatment planning

In order to investigate the efficacy of various laser-guided and image-guided target localization techniques to escalate dose, five prostate patients were analyzed as recruited in a previous study.[30] Of the five patients, three had 15 treatment CT studies and the remaining two had 16 treatment CT studies completed during their treatment course (77 studies in total). The clinical target volume (CTV) contoured in all five patients included the prostate without the seminal vesicles. The rectum and bladder were the dose-limiting organs at risk (OAR). All patients were then planned with an 18 MV, six-field conformal technique with a uniform margin size (CTV to PTV) of 10 mm. Each field was auto-shaped with a multileaf collimator (MLC) to conform to the planning target volume (PTV) and, to allow for beam penumbra, a further 8 mm was added beyond the PTV to the beam edge to generate adequate dosimetric coverage to the PTV. Each field shape was then manually fine-tuned for optimal coverage of the target as well as to meet the dose-volume criteria for the organs at risk used at our institution (RTOG P-0126).[31] Finally, dose distributions were calculated using a $3\times3\times3$ mm grid with tissue inhomogeneity and surface corrections enabled (THERAPLAN PLUS version 3.0, Nucletron, Netherlands).

For all subsequent CT studies taken during the course of treatment (termed "treatment CT images" in this paper), beam setup parameters from the planning CT data were imported onto these treatment CT images. Dose distributions were then recalculated on the treatment CT images using weighted beam normalization and were intentionally *not* renormalized to 100% at the isocenter at each fraction. This accounts for changes in tissue density and external contour of the patient from fraction to fraction, as described in our previous work (Schaly *et al.*[30]). In effect, this simulates the application of the treatment beam delivery without any adjustments of the monitor units to compensate for daily patient shape (i.e., tissue depth) changes, and hence simulates the actual treatment conditions the patients were exposed to. A previously developed and validated deformable dose tracking procedure using contour driven thin-plate splines[28,29] was then used to accumulate regional doses in the deforming tissue volumes of interest, from fraction to fraction.

B. Target localization techniques in radiation therapy

A full description of the target localization techniques investigated in this study was reported in our previous work[30] and is only briefly reviewed here. For all techniques, monitor units and MLC shapes were not reoptimized from fraction to fraction. Simply, adaptation of the interfractional geometric uncertainties was conducted by shifting the isocenter of the

beams to the best estimate of where the target was positioned on each treatment day using the particular target localization technique that was being evaluated. The subsequent calculation of dose distributions on the treatment CT images was then used for evaluation of dosimetric coverage to the daily deforming target and the variable anatomy. The following techniques were simulated and analyzed in this study.

1. Laser-guided alignment to skin tattoo marks

This technique represents a conventional treatment where skin tattoo marks are aligned to the lasers in the treatment room for daily isocenter determination and beam setup. To simulate this on the treatment CT images, the corresponding isocenter coordinates were determined from the location of metallic wires (representing the tattoo marks) placed on the patients as shown on the images. The beams were then positioned according to the coordinates of the marks and the dose distributions were calculated.

2. Image-guided alignment to bony landmarks

This technique represents another conventional localization approach of using daily portal images to guide the alignment of the beams by matching bony landmarks from the planned images to the "images of the day." To simulate this, the pelvic bones seen on each treatment CT image were registered to the planned CT image using an in-house matching algorithm.[30] Beams were then adjusted to the new isocenter coordinates determined from the bony registration and the dose distributions were calculated on the treatment CT images. Note that this technique only accounts for the setup uncertainties and does not explicitly adapt to internal organ motions since the bony landmarks are assumed only to be a surrogate representation of the actual daily prostate movements.

3. Image-guided alignment to daily CTV

Alignment of the beams to the daily CTV volume represents the most advanced target localization technique considered in this study since both the setup uncertainty and the internal organ movements are accounted for. This technique can be implemented with the use of kilovoltage (kV)[11,19] or megavoltage (MV)[18] CT images (and to a lesser extent ultrasound[23] and implanted markers[32–34]) to determine the daily target volume and its location. To simulate this technique, the center-of-mass coordinates of the prostate volume contoured on each treatment CT images were calculated and compared to the homologous coordinates of the planning CT images. Subsequently, the beams were then realigned by the vector difference of the center-of-mass coordinates between the prostate volume in the planning image to the daily instances of the prostate volume. Once the beams were setup to the new coordinates, the dose distributions were calculated on the treatment CT images.

4. Margin reduction from 10 to 5 mm

The treatment plan was redesigned with a reduced CTV to PTV margin size of 5 mm. Reducing the margin size increases normal tissue sparing and introduces the possibility for further dose escalation.[15–17] Two techniques described earlier were resimulated with the reduced margin size. First, the "alignment to daily CTV" technique was simulated because this technique was expected to significantly reduce geometric uncertainties and hence is suitable for smaller margin sizes. Second, the "alignment to skin tattoo marks" technique was also simulated to demonstrate the possible risks involved in reducing margins without having an adequate image guidance system in place to increase the precision of target localization.

C. Normalized total dose and biological outcome indices

Based on the linear quadratic model of cell survival, the normalized total dose (NTD) distribution[35] is defined as follows:

$$\mathrm{NTD}(x,y,z) = \sum_{i=1}^{N} d_i(x,y,z)\left(\frac{\frac{\alpha}{\beta} + d_i(x,y,z)}{\frac{\alpha}{\beta} + 2\ \mathrm{Gy}}\right),$$

where $d_i(x,y,z)$ is the physical dose delivered to a point at (x,y,z) in ith fraction of an N-fraction treatment. This represents the dose that a tissue volume element at (x,y,z), in the patient coordinate system of the initial treatment plan, receives according to each geometric shift and deformation during the course of treatment. This was possible since the dose received by the tissue voxels in each fraction were "back tracked" to the planning CT coordinates using the thin-plate spline based nonlinear dose warping procedure developed[28] and validated[29] by our group.

For NTD calculations, an α/β ratio of 1.5 Gy was assumed for the prostate[36,37] and α/β ratio of 3 Gy was used for both the rectum and bladder.[37,38] Once the physical dose distribution was converted to the NTD distribution for each prescription dose, the NTD dose inside the CTV and the OAR volumes were used to calculate the TCP and the NTCP, respectively. The TCP calculation was based on the model of Niemierko and Goitein,[39] where we assumed a uniform CTV clonogen density of 10^7 cm^{-3}, SF_2 of 0.50, SF_2 population standard deviation of 0.05, and SF_2 individual standard deviation of 0.03.[35] The NTCP calculation was based on the model of Lyman–Burman–Kutcher.[40–42] As suggested by Burman *et al.*,[41] a TD_{50} of 80 Gy was used for both the rectum and bladder, n of 0.12 and 0.5, and m of 0.15 and 0.11 were used for the rectum and bladder, respectively.

D. Evaluation of target localization techniques and the iso-NTCP dose escalation strategy

During treatment planning, a standard dose of 70 Gy was prescribed to the 96% isodose line in 35 fractions to optimize PTV coverage without exceeding the normal tissue criteria.

For the remaining plans on the 15 or 16 (depending on the patient) treatment CT images, a dose of 2 Gy to the same 96% isodose line is prescribed but with the beams realigned to the new isocenter coordinates that were determined by the various target localization techniques simulated.

To evaluate the performance of various target localization techniques to deliver dose, the prescription dose was varied from 50 to 100 Gy in 2 Gy-per-fraction increments, i.e., the total number of fractions was varied from 25 to 50. Since the number of treatment CT images available (15 to 16) were less than the number of actual treatment fractions simulated in this study (25 to 50), the treatment CT images were "recycled." For example, with a given prescription dose of 70 Gy (35 fractions $\times$ 2 Gy/fraction), 35 instances were randomly selected from the pool of treatment CT images for each patient. The voxel doses inside the appropriate organ volumes were then accumulated to calculate the corresponding TCP and NTCP values. At each prescription dose from 50 to 100 Gy, this process was repeated for 200 possible treatment courses (i.e., choosing 35 fractions 200 times) in order to achieve statistical stability. This way, 200 TCP and NTCP values were obtained at each prescription dose, for each target localization technique, from which averages as well as standard deviations were calculated to evaluate their performances.

The adaptive strategy employed in this work for patient-specific dose escalation was to accumulate each 2 Gy-per-fraction dose distribution in increments, delivered with each simulated target localization technique, until the rectum NTCP reached a value equal to that of the corresponding planning NTCP that was originally prescribed with 70 Gy in 35 fractions (i.e., iso-NTCP dose escalation). Therefore, the level of normal tissue sparing achieved with each target localization technique directly determined the level of dose escalation allowed. The planning NTCP values for each patient are listed in Table I below (5.9%–7.6% for 10 mm margin) and were used as the "safe limit" for dose escalation here because the plans were clinically approved for treatment. Once the escalated prescription doses were determined for each patient (unique to each target localization technique) the corresponding TCP values were calculated and recorded. In this work, only the rectum NTCP values were analyzed since the bladder NTCP values were all close to 0% and hence are insignificant to the discussions here.

TABLE I. Summary of prostate TCP and rectum NTCP values calculated for the various treatment scenarios. Mean and standard deviations of the 200 random sampling are listed for the TCP and NTCP values.

Prostate (%)	Patient 1 TCP	Patient 2 TCP	Patient 3 TCP	Patient 4 TCP	Patient 5 TCP
10 mm margin					
Planned	70.8	73.3	77.6	76.8	70.4
Tattoo registered	68.7±0.2	69.4±0.3	74.9±0.4	75.9±0.2	70.0±0.2
Bone registered	69.5±0.1	70.3±0.2	75.3±0.3	75.5±0.1	70.3±0.1
CTV registered	69.7±0.1	70.5±0.2	75.8±0.2	75.7±0.2	70.4±0.1
5 mm margin					
Planned	69.9	73.3	77.7	75.9	70.1
Tattoo registered	57.0±7.4	68.5±0.4	71.4±2.1	74.4±0.2	69.7±0.1
CTV registered	68.8±0.1	70.5±0.2	75.8±0.2	74.7±0.1	70.3±0.1
Rectum (%)	NTCP	NTCP	NTCP	NTCP	NTCP
10 mm margin					
Planned	5.9	6.6	7.6	6.9	6.6
Tattoo registered	9.0±0.6	0.9±0.2	5.5±0.7	1.1±0.2	4.6±0.5
Bone registered	7.2±0.2	2.8±0.2	9.0±0.5	5.3±0.3	5.9±0.3
CTV registered	4.1±0.1	3.1±0.1	4.0±0.2	5.7±0.2	5.2±0.2
5 mm margin					
Planned	2.6	3.2	3.7	3.3	3.5
Tattoo registered	5.4±0.6	0.2±0.1	2.8±0.5	0.2±0.1	2.2±0.4
CTV registered	1.9±0.1	1.3±0.1	1.7±0.1	2.3±0.1	2.6±0.1

III. RESULTS

Figure 1 shows the TCP (left curves) and rectum NTCP (right curves) values achieved as a function of prescription dose (ranging from 50 to 100 Gy) delivered by the various target localization techniques, for the five patients. The figure shows that the three techniques (with 10 mm margin size) and the "CTV registered" technique (with 5 mm margin size) yield nearly identical TCP curves for every patient but highly dispersed NTCP curves. Several comments can be made about the results. First, since the TCP curves are similar for the three techniques, this suggests that the 10 mm margin size was adequately large enough to accommodate the level of geometric uncertainty observed for the patients, irrespective of the target localization technique used. Second, reducing the margin size down to 5 mm while localizing the daily target volume with the "CTV registered" technique does not compromise the precision of therapy since the TCP values are not degraded relative to the 10 mm margin counterpart. Finally, for the "CTV registered" technique, reducing the margin size to 5 mm always achieves significant reduction in NTCP values. In general, the "tattoo registered" technique had the largest random variability of NTCP values (i.e., largest error bars).

Figure 2 shows the results for the "tattoo and CTV registered" techniques with the reduced margin size of 5 mm, for the five patients. Notably, for patients 1 and 3, the TCP curve is significantly degraded for the "tattoo registered" technique. In terms of NTCP however, the "tattoo registered" technique was superior for patients 2, 4, and 5.

Table I lists the average TCP and rectum NTCP values (with their standard deviations) calculated for the prescription dose of 70 Gy (35 fractions $\times$ 2 Gy/fraction), for the five patients. For both margin sizes, the "CTV registered" technique yielded TCP values that are closest to the treatment plan TCPs for the majority of patients. As noted in Fig. 1, in the case when the margin size is 10 mm, the difference in TCP values among the three techniques was generally small ($\leqslant$1%). With the reduced margin size of 5 mm, a significant reduction in TCP is seen with the "tattoo registered" technique for patients 1 and 3 (and to a lesser extent patient 2). In terms of NTCP, no single technique seemed to demonstrate a consistent and significant advantage since the

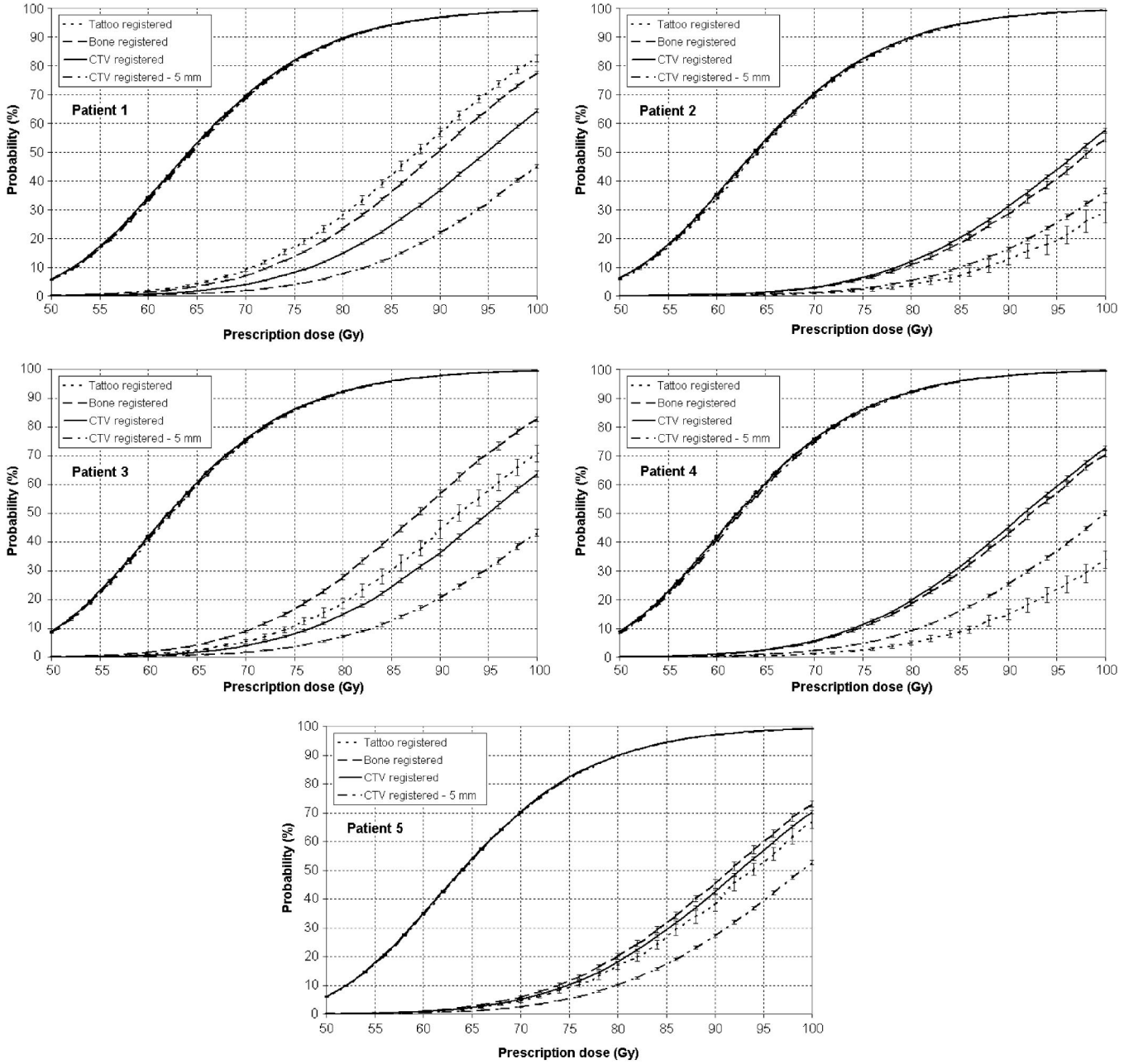

FIG. 1. The prostate TCP and rectum NTCP curves calculated as a function of dose for each patient, from 50 to 100 Gy in 2 Gy-per-fraction increments, for the three IGART techniques (i.e., tattoo, bone, and CTV registered) and the "CTV registered" technique with the reduced margin size of 5 mm. All TCP curves are on the left and all NTCP curves are on the right. Error bars are standard deviations of the 200 random histories.

corresponding technique with the lowest NTCP value was different from patient to patient. For example, in the case of patients 1 and 3, the "CTV registered" technique yielded the lowest, whereas for patients 2, 4, and 5, the "tattoo registered" technique yielded the lowest NTCP. However, a consistent and significant reduction in NTCP was always observed when the margin size was reduced from 10 to 5 mm (~60% reduction), irrespective of the techniques simulated.

Figure 3 shows the corresponding differential increase in dose ($\Delta\text{dose} = \text{dose}_{\text{technique}} - 70$ Gy) and TCP ($\Delta\text{TCP} = \text{TCP}_{\text{technique}} - \text{TCP}_{\text{plan, 70 Gy}}$) allowed by the iso-NTCP dose escalation strategy described earlier, for each patient. The figure shows that for patients 2, 4, and 5, the "tattoo registered" technique allowed the highest dose and TCP escalations for both margin sizes. For patients 1 and 3, however, the "CTV registered" technique allowed the highest dose and TCP escalations.

Table II lists the results of Fig. 3, averaged over the five patients, with standard deviations. It is seen here that the "tattoo registered" technique allowed the largest increase in dose (for both margin sizes), followed by the "CTV registered" and "bone registered" techniques. The results are due to the nature of the iso-NTCP dose escalation strategy where if the NTCP values remain sufficiently low after the 70 Gy is

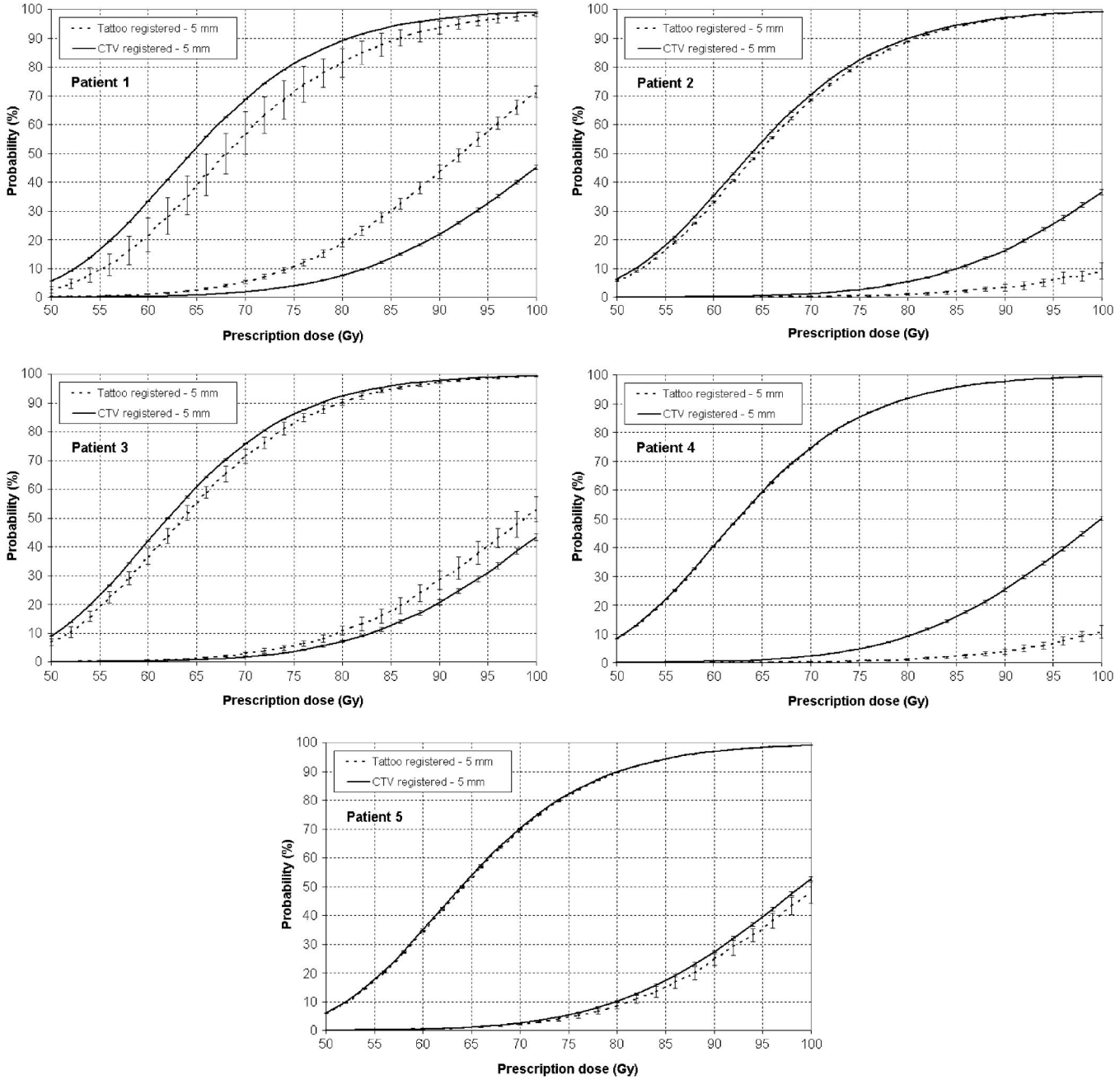

FIG. 2. The prostate TCP and rectum NTCP curves calculated as a function of dose for each patient, from 50 to 100 Gy in 2 Gy-per-fraction increments, for the two IGART techniques (i.e., tattoo and CTV registered) with the reduced margin size of 5 mm. All TCP curves are on the left and all NTCP curves are on the right. Error bars are standard deviations of the 200 random histories.

delivered, then there is an opportunity for larger dose escalation. With this in mind, recall in Table I that for patients 2 and 4, the NTCP values were much lower for the "tattoo registered" technique. This allowed large dose escalations to be permitted on the two patients (average of 14 and 26 Gy gains for 10 and 5 mm margin sizes, respectively), which increased the TCP average in Table II significantly. In the case of patient 1 though, the deliverable dose needed to be decreased below 70 Gy to meet the iso-NTCP criterion (Fig. 3). This caused a large standard deviation observed for this technique (Table II). In terms of the corresponding TCP gain, the "tattoo registered" (7.5%) and "CTV registered" (15.3%) techniques yielded the highest values for the 10 and 5 mm margin sizes, respectively. The smallest standard deviations, in terms of dose and TCP escalations for the five patients, were observed with the "CTV registered" technique, for both margin sizes.

IV. DISCUSSION

A. General comments

The current work is part of a continued effort to evaluate the impact of various IGART techniques on the outcome of radiation treatments using a dose warping procedure.[28–30]

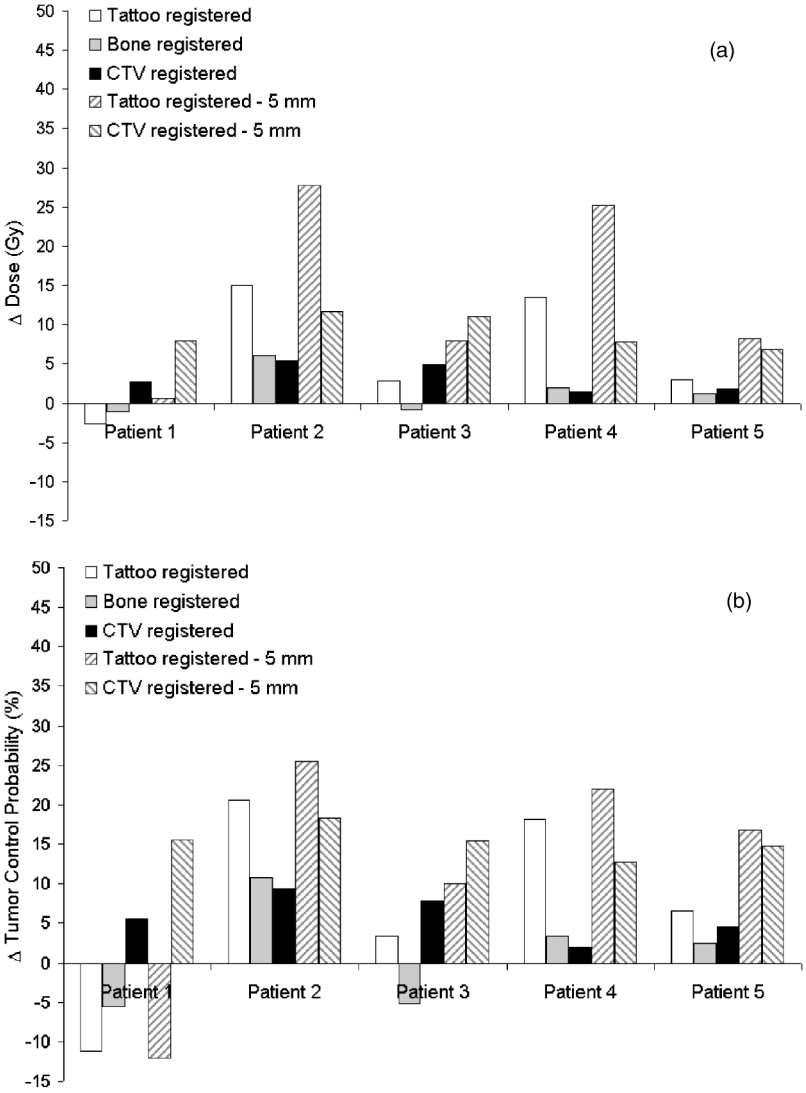

FIG. 3. Histogram of the theoretical iso-NTCP differential (a) dose and the corresponding (b) TCP escalations allowed by the various strategies evaluated in this study. For patients 1 and 3, the "CTV registered" technique allowed the highest dose and TCP escalations for both margin sizes. For patients 2, 4, and 5, however, the "tattoo registered" technique allowed the highest dose and TCP escalations.

Specifically, the work presented here focused on potential dose escalations allowed with the assistance of various target localization technologies. This is particularly important since it is becoming established that prostate cancer local control improves with higher doses.[2–6] Dose escalation, however, must be accompanied by an adequate sparing of normal tissues. Reducing the margin size effectively accomplishes this but at the expense of greater uncertainty in dosimetric coverage to the target. Hence, it seems advisable that any margin reduction scheme should be accompanied by an advanced image guidance system throughout the course of treatment.

TABLE II. Summary of the average iso-NTCP differential dose and TCP escalations allowed by the various strategies evaluated in this study. Mean and standard deviations of the five patients are listed for the Δ Dose and Δ TCP.

	Δ Dose(Gy)	Δ TCP(%)
10 mm margin		
Tattoo registered	6.4±7.6	7.5±13
Bone registered	1.5±2.9	1.2±6.8
CTV registered	3.3±1.8	5.8±2.9
5 mm margin		
Tattoo registered	14.0±12	12.5±15
CTV registered	9.1±2.1	15.3±2.0

Orton *et al.*[23] recently reviewed the dosimetric impact of localizing the daily prostate volume with the transabdominal ultrasound when the margin size was reduced to 5 mm. They found that the dose distributions to targets and critical structures for post plans incorporating the daily shifts (analogous to the "CTV registered" technique in this paper) are nearly identical to those of the treatment plan. But, when no shifts were made to their initial setup (analogous to the "tattoo registered" technique in this paper), the TCP values reduced significantly (up to 10% from plan). This is similar to the findings of our work for the 5 mm margin case where two of the five patients showed significant reductions in TCP with the "tattoo registered" technique (up to 13% from plan for 5 mm margin, Table I). But, for the "CTV registered" technique, the TCP values were all close to the treatment plan TCPs for both margin sizes ($\leqslant$2.8% difference, Table I). For the 10 mm margin case, however, the "tattoo registered"

technique did not yield a large TCP degradation for any patient either ($\leqslant$3.9% difference, Table I). Thus, at least for the margin sizes as small as 5 mm should be carefully used in conjunction with the conventional "tattoo registered" technique when treating prostate cancer since the technique may be susceptible to both the setup and organ motion uncertainties in some patients.

Recently, Ghilezan *et al.*[43] published a theoretical study assessing the clinical benefits and potential dose escalation allowed by the on-line utilization of an onboard cone-beam CT (analogous to the "CTV registered" technique in this paper) system to correct for interfractional geometric uncertainties. Twenty-two prostate patients were retrospectively simulated both with conventional IMRT (with margin of 1 cm) and on-line image-guided IMRT (with 0 cm CTV-PTV margin) techniques. Using the generalized equivalent uniform dose (EUD) as the clinical outcome indicator, they found that the standard deviation of the target EUDs of the 22 patients were significantly different between the two techniques (5.6% for conventional IMRT and 0.7% for online image-guided IMRT). This suggested that the image-guided technique provided superior consistency in delivering the intended dose from patient to patient. This finding is similar with the results of our study where the "CTV registered" technique provided a higher TCP (i.e., closer to the plan TCP) for the majority of patients, as compared to the conventional "tattoo registered" technique for both the 10 and 5 mm margin scenarios (Table I). Ghilezan *et al.* also found that the benefit of using online CT image guidance for dose escalation was highly patient-dependent and that, on average, a target dose increase of 13% (9.7% SD) could be achieved with the constraint of the dose-limiting rectum. In our study, the "CTV registered" technique with the 5 mm margin size allowed a similar increase in target dose where an increase of 9.1 Gy was allowed (i.e., 13% increase from 70 Gy, Table II). However, in contrast to their study, the laser-guided "tattoo registered" technique yielded the largest average increase in dose (i.e., 14.0 Gy increase, Table II) in our study.

The geometric localization techniques investigated in this study did not include daily monitor units and MLC updates to account for interfractional patient shape changes (e.g., weight loss/gain and target deformations). The effect of this on the treatment outcome was small but not negligible (i.e., $\text{effect} \approx \text{TCP}_{\text{plan}} - \text{TCP}_{\text{CTV registered treatment}}$). This is evident in Table I where the planning TCP values are generally larger than the TCP values of the "CTV registered" treatments ($\leqslant$2.8%). The reason, however, for not adapting monitor units and MLC shapes in this study was that such a level of adaptation can only be employed with the "CTV registered" technique. In order to accurately update for monitor units and MLC shapes, the isocenter location relative to the CTV as well as three-dimensional target volumetric information are required daily. This level of information is only available with the daily treatment CT images and hence cannot be incorporated into the "tattoo and bone registered" techniques. Since our primary interest in this study was to quantify the effects of daily target localization by various laser-guided and image-guided techniques, all conditions were kept constant and in accordance with the current clinical practice for an unbiased comparison. However, optimizing for monitor units and MLC shapes represent an obvious next step in the adaptation of geometric uncertainties, this will be investigated in the future.

In this study, the comparison of various IGART techniques was confined to a single beam delivery method, namely, the six-field co-planar treatment. Other treatment methods, such as intensity modulated radiation therapy (IMRT),[43] which would result in different levels of normal tissue sparing, combined with the IGART investigated here may have allowed higher dose escalations than the six-field technique.[13,14] This will be explored in the future, however, with the IMRT-dedicated tomotherapy unit recently installed at our institution (TomoTherapy HiART, TomoTherapy Inc., Madison WI). Once the tomotherapy unit is fully functional and daily MVCT images are available, more sophisticated IGART strategies other than the daily isocenter shifts with iso-NTCP dose escalation (explored in this study) can be investigated as well. They include reoptimization of treatment margins,[14,22] reoptimization of prescription dose[14,18] (similar to the work done in this study with an iso-NTCP constraint or other dosimetric constraints), and reoptimization of the entire plan using dose-volume based objective functions with inverse planning.[18,24–26,43] The best way to adapt using feedback of images is currently under active research and it is to be determined which technique will be the most optimal in terms of clinical outcome as well as in terms of practical logistics.

Finally, the dose escalation strategy adopted in this work increased the prescription dose in 2 Gy-per-fraction increments. There are alternative ways to escalate dose that were not explored in this study such as increasing the dose-per-fraction size while keeping the total fraction numbers constant or the combination of increasing both. There were two reasons for this. First, escalating the dose in $\sim$2 Gy-per-fraction increments is becoming established as an effective method of improving prostate tumor response.[2–6] Second, predicting the outcome of treatment schedules that varies in dose-per-fraction size (e.g., hypofractionation or hyperfractionation) is challenging to model radiobiologically since the outcome is sensitive to the prostate α/β ratio, the value of which is under a heated debate[36,37,44] at this time. However, because such a strategy has significant implications for radiation therapy[45] this topic will be explored in a future study.

B. Implications of the results

Table III lists the summary of published literature on prostate motion and setup errors as compared to our observations in five patients. It is seen here that the overall population average for prostate motion in our data set is comparable to the literature, in all three directions (i.e., lateral, anterior-posterior, and superior-inferior). The typical directional trend of larger prostate motion in the AP and SI directions as compared to the lateral direction is also observed. However, this

TABLE III. Summary of published literature on prostate motion and set-up errors as compared to the observed data in the current study. Population means and one standard deviations (in parentheses), in each direction, are listed.

	Prostate motion		
Author	LAT (mm)	AP (mm)	SI (mm)
Song *et al.* (current work)	−0.4(0.6)	3.3 (3.7)	0.9 (2.0)
Vigneault *et al.*[a]	1.4 (1.4)	2.7 (2.3)	3.0 (2.1)
Crook *et al.*[b]	0.5 (1.5)	−6.0(4.1)	−5.9(5.0)
Wu *et al.*[c]	N/A	0.7 (2.3)	0.6 (2.1)
	Set-up error		
	LAT (mm)	AP (mm)	SI (mm)
Song *et al.* (current work)	−0.5(6.9)	1.6 (5.7)	−0.7(3.2)
Vigneault *et al.*[a]	1.7 (2.1)	2.0 (2.5)	1.9 (2.5)
Bel *et al.*[d]	0.3 (2.0)	0.9 (1.7)	−0.9(1.8)
Millender *et al.*[e]	11.4 (1.2)	2.6 (0.4)	7.2 (0.9)

[a]Reference 32.
[b]Reference 33.
[c]Reference 34.
[d]Reference 47.
[e]Reference 46.

was not the case with the set-up error, where comparably larger variations (standard deviations) were found. This was due in large part to patient 2, who was very large in size and caused the anterior skin tattoo mark to "wobble" significantly (10.1 mm average, lateral) from fraction to fraction. However, set-up deviations of larger (obese) patients were recently studied by Millender *et al.*[46] and they report similar findings to patient 2 of our study (11.6 mm for three patients, lateral). Thus, the five prostate cancer patients selected for the current study represent a good sample compared to a larger population reported elsewhere.[32–34,46,47]

The results of this work demonstrated that the "CTV registered" technique, which corrects for interfractional CTV movements, did not always allow for the highest dose escalations. The best IGART technique to use for dose escalation was in fact patient dependent. In three out of five patient cases, the "tattoo registered" technique allowed the highest iso-NTCP dose escalations. But, the caveat to this finding was that the amount of permitted dose increase was highly inconsistent from patient to patient and that, at this time, no reliable "predictive" indicator exists that can determine which patients would benefit most from iso-NTCP dose escalation with the "tattoo registered" technique prior to their treatments. As seen in Table II, the standard deviation in dose escalations among the five patients was very large and comparable to the actual dose gain (i.e., 6.4 ± 7.6 Gy and $7.5\pm13\%$ for dose and TCP increases, respectively, for the 10 mm margin). As well, when the margin size was reduced to 5 mm, this technique did not as efficiently translate the increase in dose to an increase in tumor control as compared to the "CTV registered" technique (i.e., increase of 14.0 Gy resulted in TCP increase of only 12.5 %, Table II). This was due mainly to the fact that, in general, when the rectum volume was inadvertently spared by the beam placements with the "tattoo registered" technique, the target coverage was also compromised in many instances. For example, with an anterior set-up error, the beams are placed away from the rectum volume (achieving a significant sparing of rectum) but at the same time missing a significant posterior portion of the prostate volume (compromising the target coverage) due to the use of an inadequately small margin size (i.e., 5 mm). With the "CTV registered" technique, though, the anterior setup error would be remedied in this case by moving the beams posteriorly (achieving an adequate target coverage) but irradiating more rectum volume (compromising the rectum sparing) as a consequence. Hence, the "tattoo registered" technique may be unreliable for dose escalation purposes since a consistent dosimetric coverage to the target cannot be assured from patient to patient with smaller margin sizes (e.g., 5 mm), where a greater opportunity exists for larger dose escalations. This point is especially important in light of the fact that many dose escalation studies performed to date have used "tattoo registered" technique, without image guidance, with 5 mm margin at the interface between the prostate and rectum. Thus, without some sort of image guidance, clinical studies using small margins and tattoo registration techniques may run the risk of underestimating the potential benefits of dose escalation.

In contrast, the "CTV registered" technique translated the increase in dose to an increase in tumor control more efficiently (i.e., increase of 9.1 Gy resulted in TCP increase of 15.3%, Table II), meaning that the extra dose prescribed was all accurately delivered to the prostate volume. This was consistently observed from patient to patient which resulted in the lowest variation in dose and TCP increases allowed for the patient population (in terms of standard deviations listed in Table II) among the techniques simulated. The "CTV registered" technique was the only technique in which positive iso-NTCP dose escalation (i.e., $\geqslant$70 Gy) was allowed on all five patients (Fig. 3). Even when the margin size was reduced to 5 mm, the standard deviation of the dose escalations calculated remained comparable to the 10 mm margin counterpart (1.8 vs 2.1 Gy), but with almost a triple the increase in dose (3.3 vs 9.1 Gy) and TCP (5.8 vs 15.3%). Therefore, the dose escalation trials accompanied by the "CTV registered" technique would best ensure a consistent and reliable target coverage for the patient population, which, in our opinion, is one of the most important prerequisites for any successful clinical trials. The "bone registered" technique was more consistent in terms of dose escalation than the "tattoo registered" technique for the 10 mm margin size also but did not, in general, achieve high enough dose escalations for significant TCP gains (i.e., 1.5 ± 2.9 Gy and $1.2\pm6.8\%$ for dose and TCP increases, respectively).

The impact of image guidance technology on normal tissue sparing was not as predictable as it was for the target. The dose received, and hence NTCP, by the rectum with the guidance of "tattoo, bone and CTV registered" techniques was patient specific, as it depended on the interplay between setup error and organ motion as well as the shape of the dose distribution created by the six-field beam delivery method. That is, the six-field plan, implemented in this study, produces diamond-shaped dose distribution that is elongated lat-

erally. Hence the plan tends to be more robust against lateral shifts than anterior-posterior or superior-inferior shifts of the target. On occasion, correcting for the lateral shifts of the target using the "CTV registered" technique inadvertently places the rectum back into the high dose region, as well. Therefore, we observed that the dose received by the rectum in each fraction depended heavily on the rectum shape and the image guidance system used for the target localization. Thus, in general for all patients, the magnitude of normal tissue sparing depended significantly more on the amount of CTV to PTV margin reduction than the actual target localization technique used. For example, it was shown in Table I that, on average, the margin reduction from 10 to 5 mm resulted in ~60% decrease in rectum NTCP for both the "tattoo and CTV registered" techniques for the prescription dose of 70 Gy. Therefore, the optimal dose escalation strategy seems to be to combine margin reduction (for increased normal tissue sparing) with the use of "CTV registered" technique to localize the daily target volume (for consistent dosimetric coverage). In addition, a normal tissue immobilization device such as rectal balloon[48] may further spare the rectum by reducing the geometric variation and by decreasing the absolute volume receiving the high dose. However, it remains to be verified clinically whether such devices will actually lower the occurrence of normal tissue damage in long run.

V. CONCLUSION

In general, the CT image guidance technology will enable safe and consistent dose escalation for the patient population by improving the precision of dose delivery in individual multifraction treatments. Specifically, based on the data analyzed in this study, we conclude that:

(1) the selection of the IGART techniques was less critical on the treatment outcome when generous margins are used ($\geqslant$10 mm);
(2) reducing the margin size from 10 to 5 mm generally increased the normal tissue sparing but no IGART technique showed significant advantage over the others in this respect;
(3) the conventional "tattoo registered" technique was inadequate, in terms of TCP, to correct for daily geometric uncertainties when the margin size was reduced to 5 mm;
(4) an attractive dose escalation strategy for clinical use may be to combine margin reduction (for high normal tissue sparing) with the use of "CTV registered" technique to localize the daily target volume (for consistent dosimetric coverage).

ACKNOWLEDGMENTS

The funding for this research was provided by CIHR Strategic Training Initiative in Cancer Research and Technology Transfer and Ontario Graduate Scholarship in Science and Technology (OGSST).

[a]Electronic mail: william.song@lrcc.on.ca

[1]J. M. Michalski, "Introduction: Locally advanced prostate cancer," Semin. Radiat. Oncol. **13**, 85–86 (2003).
[2]A. I. Blanco and J. M. Michalski, "Dose escalation in locally advanced carcinoma of the prostate," Semin. Radiat. Oncol. **13**, 87–97 (2003).
[3]E. H. Huang *et al.*, "Late rectal toxicity: Dose-volume effects of conformal radiotherapy for prostate cancer," Int. J. Radiat. Oncol., Biol., Phys. **54**, 1314–1321 (2002).
[4]G. E. Hanks *et al.*, "Dose escalation with 3D conformal treatment: Five year outcomes, treatment optimization, and future directions," Int. J. Radiat. Oncol., Biol., Phys. **41**, 501–510 (1998).
[5]M. J. Zelefsky *et al.*, "Dose escalation with three dimensional conformal radiation therapy affects the outcome in prostate cancer," Int. J. Radiat. Oncol., Biol., Phys. **41**, 491–500 (1998).
[6]M. J. Zelefsky *et al.*, "High-dose intensity modulated radiation therapy for prostate cancer: Early toxicity and biochemical outcome in 772 patients," Int. J. Radiat. Oncol., Biol., Phys. **53**, 1111–1116 (2002).
[7]M. van Herk, A. Bruce, G. Kroes, T. Shouman, A. Touw, and J. V. Lebesque, "Quantification of organ motion during conformal radiotherapy of the prostate by three-dimensional (3D) image registration," Int. J. Radiat. Oncol., Biol., Phys. **33**, 1311–1320 (1995).
[8]J. C. Stroom *et al.*, "Internal organ motion in prostate cancer patients treated in prone and supine treatment position," Radiother. Oncol. **51**, 237–248 (1999).
[9]J. M. Balter *et al.*, "Measurement of prostate movement over the course of routine radiotherapy using implanted markers," Int. J. Radiat. Oncol., Biol., Phys. **31**, 113–118 (1995).
[10]J. M. Crook *et al.*, "Prostate motion during standard radiotherapy as assessed by fiducial markers," Radiother. Oncol. **37**, 35–42 (1995).
[11]D. A. Jaffray, J. H. Siewerdsen, J. W. Wong, and A. A. Martinez, "Flat-panel cone-beam computed tomography for image-guided radiation therapy," Int. J. Radiat. Oncol., Biol., Phys. **53**, 1337–1349 (2002).
[12]D. Yan, F. Vicini, J. Wong, and A. Martinez, "Adaptive radiation therapy," Phys. Med. Biol. **42**, 123–132 (1997).
[13]L. Happersett *et al.*, "A study of the effects of internal organ motion on dose escalation in conformal prostate treatments," Radiother. Oncol. **66**, 263–270 (2003).
[14]A. A. Martinez *et al.*, "Improvement in dose escalation using the process of adaptive radiotherapy combined with three-dimensional conformal or intensity-modulated beams for prostate cancer," Int. J. Radiat. Oncol., Biol., Phys. **50**, 1226–1234 (2001).
[15]M. Engelsman, P. Remeijer, M. van Herk, J. V. Lebesque, B. J. Mijnheer, and E. M. F. Damen, "Field size reduction enables Iso-NTCP escalation of tumor control probability for irradiation of lung tumors," Int. J. Radiat. Oncol., Biol., Phys. **51**, 1290–1298 (2001).
[16]M. Engelsman, P. Remeijer, M. van Herk, B. J. Mijnheer, and E. M. F. Damen, "The theoretical benefit of beam fringe compensation and field size reduction for iso-normal tissue complication probability dose escalation in radiotherapy of lung cancer," Med. Phys. **30**, 1086–1095 (2003).
[17]W. Song and P. Dunscombe, "EUD-based margin selection in the presence of set-up uncertainties," Med. Phys. **31**, 849–859 (2004).
[18]T. R. Mackie *et al.*, "Image guidance for precise conformal radiotherapy," Int. J. Radiat. Oncol., Biol., Phys. **56**, 89–105 (2003).
[19]M. Uematsu *et al.*, "Focal, high dose, and fractionated modified stereotactic radiation therapy for lung carcinoma patients: A preliminary experience," Cancer **82**, 1062–1070 (1998).
[20]L. E. Court and L. Dong, "Automatic registration of the prostate for computed-tomography-guided radiotherapy," Med. Phys. **30**, 2750–2757 (2003).
[21]M. H. P. Smitsmans, J. W. H. Wolthaus, X. Artignan, J. De Bois, D. A. Jaffray, J. V. Lebesque, and M. van Herk, "Automatic localization of the prostate for on-line or off-line image-guided radiotherapy," Int. J. Radiat. Oncol., Biol., Phys. **60**, 623–635 (2004).
[22]D. Yan, D. Lockman, D. Brabbins, L. Tyburski, and A. Martinez, "An off-line strategy for constructing a patient-specific planning target volume in adaptive treatment process for prostate cancer," Int. J. Radiat. Oncol., Biol., Phys. **48**, 289–302 (2000).
[23]N. P. Orton and W. A. Tome, "The impact of daily shifts on prostate IMRT dose distributions," Med. Phys. **31**, 2845–2848 (2004).
[24]C. Wu, R. Jeraj, G. H. Olivera, and T. R. Mackie, "Re-optimization in adaptive radiotherapy," Phys. Med. Biol. **47**, 3181–3195 (2002).
[25]C. Wu, R. Jeraj, W. Lu, and T. R. Mackie, "Fast treatment plan modifi

cation with an over-relaxed Cimmino algorithm," Med. Phys. **31**, 191–200 (2004).
[26]M. Birkner, D. Yan, M. Alber, J. Liang, and F. Nusslin, "Adapting inverse planning to patient and organ geometrical variation: Algorithm and implementation," Med. Phys. **30**, 2822–2831 (2003).
[27]D. Brabbins *et al.*, "A dose escalation trial with the adaptive radiotherapy process as a delivery system in localized prostate cancer: Analysis of chronic toxicity," Int. J. Radiat. Oncol., Biol., Phys. **61**, 400–408 (2005).
[28]B. Schaly, J. A. Kempe, G. S. Bauman, J. J. Battista, and J. Van Dyk, "Tracking the dose distribution in radiation therapy by accounting for variable anatomy," Phys. Med. Biol. **49**, 791–805 (2004).
[29]B. Schaly, G. S. Bauman, J. J. Battista, and J. Van Dyk, "Validation of contour-driven thin-plate splines for tracking fraction-to-fraction changes in anatomy and radiation therapy dose mapping," Phys. Med. Biol. **50**, 459–475 (2005).
[30]B. Schaly, G. S. Bauman, W. Song, J. J. Battista, and J. Van Dyk, "Dosimetric impact of geometric adaptive radiation therapy," Phys. Med. Biol. (in press).
[31]J. Michalski, J. Purdy, D. Watkins-Bruner, and M. Amin, "A phase III randomized study of high dose 3D-CRT/IMRT versus standard dose 3D-CRT/IMRT in patients treated for localized prostate cancer," Radiation Therapy Oncology Group, Website (www.rtog.org, 2002).
[32]E. Vigneault, J. Pouliot, J. Laverdiere, J. Roy, and M. Dorion, "Electronic portal imaging device detection of radioopaque markers for the evaluation of prostate position during megavoltage irradiation: A clinical study," Int. J. Radiat. Oncol., Biol., Phys. **37**, 205–212 (1997).
[33]J. M. Crook, Y. Raymond, D. Salhani, H. Yang, and B. Esche, "Prostate motion during standard radiotherapy as assessed by fiducial markers," Radiother. Oncol. **37**, 35–42 (1995).
[34]J. Wu, T. Haycocks, H. Alasti, G. Ottewell, N. Middlemiss, M. Abdolell, P. Warde, A. Toi, and C. Catton, "Positioning errors and prostate motion during conformal prostate radiotherapy using on-line isocentre set-up verification and implanted prostate markers," Radiother. Oncol. **61**, 127–133 (2001).
[35]W. Song, J. Battista, and J. Van Dyk, "Limitations of a convolution method for modeling geometric uncertainties in radiation therapy: The radiobiological dose-per-fraction effect," Med. Phys. **31**, 3034–3045 (2004).
[36]D. J. Brenner and E. J. Hall, "Fractionation and protraction for radiotherapy of prostate carcinoma," Int. J. Radiat. Oncol., Biol., Phys. **43**, 1095–1101 (1999).
[37]J. F. Fowler, R. J. Chappell, and M. A. Ritter, "Is the α/β for prostate tumors really low?," Int. J. Radiat. Oncol., Biol., Phys. **50**, 1021–1031 (2001).
[38]J. F. Fowler, "Review article: The linear-quadratic formula and progress in fractionated radiotherapy," Br. J. Radiol. **62**, 679–694 (1989).
[39]A. Niemierko and M. Goitein, "Implementation of a model for estimating tumor control probability for an inhomogeneously irradiated tumor," Radiother. Oncol. **29**, 140–147 (1993).
[40]J. T. Lyman and A. B. Wolbarst, "Optimization of radiation therapy. IV. A dose-volume histogram reduction algorithm," Int. J. Radiat. Oncol., Biol., Phys. **17**, 433–436 (1989).
[41]C. Burman, G. J. Kutcher, B. Emami, and M Goitein, "Fitting of normal tissue tolerance data to an analytic function," Int. J. Radiat. Oncol., Biol., Phys. **21**, 123–135 (1991).
[42]G. J. Kutcher, C. Burman, L. Brewster, M. Goitein, and R. Mohan, "Histogram reduction method for calculating complication probabilities for three-dimensional treatment planning evaluations," Int. J. Radiat. Oncol., Biol., Phys. **21**, 137–146 (1991).
[43]M. Ghilezan, D. Yan, J. Liang, D. Jaffray, J. Wong, and A. Martinez, "Online image-guided intensity-modulated radiotherapy for prostate cancer: How much improvement can we expect? A theoretical assessment of clinical benefits and potential dose escalation by improving precision and accuracy of radiation delivery," Int. J. Radiat. Oncol., Biol., Phys. **60**, 1602–1610 (2004).
[44]A. E. Nahum, B. Movsas, E. M. Horwitz, C. C. Stobbe, and J. D. Chapman, "Incorporating clinical measurements of hypoxia into tumor local control modeling of prostate cancer: Implications for the alpha/beta ratio," Int. J. Radiat. Oncol., Biol., Phys. **57**, 391–401 (2003).
[45]J. F. Fowler, M. A. Ritter, R. J. Chappell, and D. J. Brenner, "What hypofractionated protocols should be tested for prostate cancer?," Med. Phys. **56**, 1093–1104 (2003).
[46]L. E. Millender, M. Aubin, J. Pouliot, K. Shinohara, and M. Roach, "Daily electronic portal imaging for morbidly obese men undergoing radiotherapy for localized prostate cancer," Int. J. Radiat. Oncol., Biol., Phys. **59**, 6–10 (2004).
[47]A. Bel, P. H. Vos, P. T. R. Rodrigus, C. L. Creutzberg, A. G. Visser, J. C. Stroom, and J. V. Lebesque, "High-precision prostate cancer irradiation by clinical application of an offline patient setup verification procedure, using portal imaging," Int. J. Radiat. Oncol., Biol., Phys. **35**, 321–332 (1996).
[48]R. R. Patel, N. Orton, W. A. Tome, R. Chappell, and M. A. Ritter, "Rectal dose sparing with a balloon catheter and ultrasound localization in conformal radiation therapy for prostate cancer," Radiother. Oncol. **67**, 285–294 (2003).